Ferromagnetic materials under high pressure in a diamond-anvil cell: A magnetic study*

Wang Xin(王 鑫)[a)b)], Hu Tian-Li(胡天立)[a)], Han Bing(韩 冰)[a)†], Jin Hui-Chao(靳会超)[a)], Li Yan(李 岩)[a)b)], Zhou Qiang(周 强)[a)b)], and Zhang Tao(张 涛)[a)‡]

[a)] *College of Physics, Jilin University, Changchun* 130012, *China*

[b)] *State Key Laboratory of Superhard Materials, Jilin University, Changchun* 130012, *China*

(Received 10 March 2014; revised manuscript received 24 April 2014; published online 29 May 2014)

A magnetic-parameter measurement system for study of ferromagnetic materials under high pressure using a diamond-anvil cell is built. The factors affecting the measurement sensitivity are analyzed and the possibility of improving the sensitivity is mentioned. Based on the system, the magnetization curves of iron as a function of pressure are obtained. The start point and end point of pressure-induced magnetic transition of iron are observed at room temperature.

Keywords: iron, high pressure, magnetic transition, magnetization curve

PACS: 52.70.Ds, 07.35.+k 62.50.–p 75.30.Kz **DOI:** 10.1088/1674-1056/23/7/070701

1. Introduction

Recently, the study of physical properties of materials under high pressure is an active research field. With the increase of pressure, the distance between the atoms of materials changes markedly, and sometimes materials undergo a phase transition.[1] The diamond-anvil cell (DAC) is the most powerful and pervasive high-pressure device. It helps researchers discover many novel phenomena concerning the behavior of materials under high pressure.[2–4] The research into the magnetic properties of materials using DACs is generally based on the inductive method to measure alternating current (AC) susceptibility, while some laboratories have developed various techniques and built diverse systems.[5–11] We have built a system to measure the magnetic transition of ferromagnetic materials. Our previous experiments obtained the variation curves of the magnetic susceptibility of iron, and the $\alpha \rightarrow \varepsilon$ phase transition of iron at room temperature is verified.[11]

Ferromagnetic materials have unique magnetic properties that not only show a high susceptibility but also display hysteresis under an external applied magnetic field. As a typical ferromagnetic material, iron has at least six phases at high pressure and temperature,[12] and there are two stable phases at room temperature: α-iron (bcc) and ε-iron (hcp). Normally α-iron transforms to ε-iron under high pressure, and the pressure and properties of this transition have been researched through numerous theoretical studies,[13–18] Mössbauer spectroscopy,[19–21] and synchrotron radiation.[22–26] The transition appears above 10–13 GPa as computed in the generalized gradient approximation.[13,15,17] Mössbauer spectroscopy investigations at room temperate find that above 13 GPa a seventh line appears near the center of the spectrum due to the phase transition, and the transition extends to about 20 GPa.[19,20] The data of X-ray absorption spectroscopy and X-ray circular dichroism give a narrower pressure domain of the structural transition (2.4 ± 0.2 GPa).[22,26] The motion of iron particles at 16.9 GPa and 261 °C in response to an external magnet suggests that hcp iron is either paramagnetic or ferromagnetic.[27]

Here we present our novel system to measure the magnetization curve of iron under high pressure. The shape of the magnetization curve gives detailed information on the magnetic parameters and also shows the process of magnetization. When pressure increases on ferromagnetic materials, the shapes of magnetization curves measured under different pressures reveal variations in saturation magnetization (M_s). The data of this experiment verify the pressure and pressure domain of the α-iron to ε-iron transition.

2. Design and theory

To measure the magnetization curves of iron under different pressures, a measurement system based on a DAC has been built. The principle of the system is based on Faraday's law. Figure 1 is a schematic view of the system. The system employs three coils, namely, the exciting coil, the pick-up coil and the compensating coil whose specification is the same as the pick-up coil, except in winding direction. The pick-up coil is mounted above the diamond whose anvil is close to the sample and the compensating coil is placed parallel with it. The exciting coil, which is driven by a voltage source to produce an ac magnetic field, is fixed around the pick-up and compen-

*Project supported by the Open Project of State Key Laboratory of Superhard Materials of Jilin University, China (Grant No. 201106).

†Corresponding author. E-mail: han@jlu.edu.cn

‡Corresponding author. E-mail: zhangt@jlu.edu.cn

© 2014 Chinese Physical Society and IOP Publishing Ltd

sating coils. The electromagnet applies a direct current (DC) magnetic field whose direction parallels the axis of pick-up coil. The pick-up coil and compensating coil are connected in series and the output voltage is measured by a lock-in amplifier (LIA).

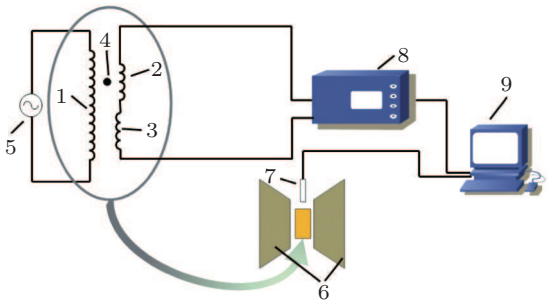


Fig. 1. (color online) Schematic view of the measurement system: (1) exciting coil; (2) pick-up coil; (3) compensation coil; (4) sample; (5) voltage source; (6) electromagnet; (7) gauss meter; (8) lock-in amplifier; and (9) computer.

Limited by the experimental conditions, the diameter of the high-pressure sample is less than 150 μm, leading to a poor signal-noise ratio. To measure the magnetization curve, it is necessary to analyze the factors affecting the output voltage of the sample to improve the measurement sensitivity. Considering the situation shown in Fig. 2, the Cartesian coordinate system o–XYZ is a static system. The center of a single layer pick-up coil is at Q (0, 0, h) and the coil is parallel to the o–XY plane.

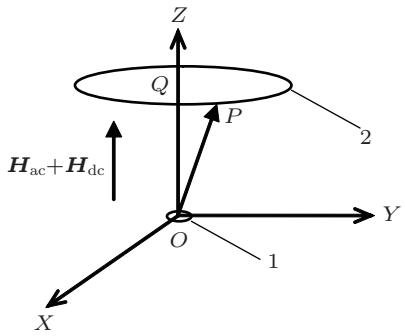


Fig. 2. Cartesian coordinate system o–XYZ: (1) current loop $\boldsymbol{m}$; (2) pick-up coil.

In comparison to the pick-up coil, the size of the sample is small enough, thus it can be equivalent to a current loop whose magnetic moment is $\boldsymbol{m}$, which depends on the shape, size and properties of the sample and the applied magnetic field. The center of this current loop is at o (0, 0, 0) and $\boldsymbol{m}$ has the identical direction with the Z axis. We assume that the AC magnetic field $\boldsymbol{H}_{ac}$ produced by the exciting coil and the external DC magnetic field $\boldsymbol{H}_{dc}$ applied by the electromagnet are uniform. Their directions are the same as $\boldsymbol{m}$. For arbitrary point $P(x, y, z)$ on the pick-up coil, the magnetic induction $\boldsymbol{B}(P)_z$ produced by $\boldsymbol{m}$ along the Z axis is

$$\boldsymbol{B}(P)_z = \frac{\mu_0}{4\pi}\frac{2z^2-x^2-y^2}{(x^2+y^2+z^2)^{5/2}}\boldsymbol{m},$$

where μ_0 is the magnetic permeability of vacuum. The definition of magnetization intensity is $\boldsymbol{M} = \sum \boldsymbol{m}/v$. Therefore, $\boldsymbol{m} = \boldsymbol{M}v = \chi \boldsymbol{H}\ v$, where v is the volume of the sample, χ is the magnetic susceptibility of the sample and $\boldsymbol{H}$ is the external magnetic field around the sample. The effective magnetic flux φ_m produced by $\boldsymbol{m}$ through the single pick-up coil can be given by

$$\varphi_m = \iint \boldsymbol{B}_z \cdot \mathrm{d}\boldsymbol{s} = \frac{\mu_0}{2}\frac{R^2\chi v}{(h^2+R^2)^{3/2}}H,$$

where s and R are the area and the radius of the single-turn pick-up coil.

The magnetic moment $\boldsymbol{m}$, $\boldsymbol{H}_{ac}$, and $\boldsymbol{H}_{dc}$ impact the magnetic flux through the single turn pick-up coil so this magnetic flux is

$$\begin{aligned}\varphi &= \varphi_m + \iint (\mu_0 \boldsymbol{H}_{ac} + \mu_0 \boldsymbol{H}_{dc}) \cdot d\boldsymbol{s} \\ &= \frac{\mu_0}{2}\frac{R^2\chi v}{(h^2+R^2)^{3/2}}(H_{ac}+H_{dc}) + \mu_0\pi R^2(H_{ac}+H_{dc}).\end{aligned}$$

If point P is on the n'-th turn of the pick-up coil, then $R = R_{in} + n'D$, where R_{in} is the inner radius of the pick-up coil and D is the diameter of the copper wire. The magnetic flux through the pick-up coil is

$$\begin{aligned}\Phi &= \sum_{n'=1}^{N}\left(R_{in}+n'D\right)^2(H_{ac} \\ &\quad + H_{dc})\frac{\mu_0}{2}\left(\frac{\chi v}{(h^2+(R_{in}+n'D)^2)^{3/2}} + 2\pi\right),\end{aligned}$$

where N is the number of turns of pick-up coil.

When a small AC magnetic field is superimposed on a large DC magnetic field, the magnetization process does not adhere to the magnetization curve but follows an incremental loop whose center is the DC magnetic field. The slope of the incremental loop $\Delta M/\Delta H$ is called incremental susceptibility χ_{inc} which depends on $\boldsymbol{H}_{ac}$ and $\boldsymbol{H}_{dc}$. If $\boldsymbol{H}_{ac}$ is small enough relative to $\boldsymbol{H}_{dc}$, χ_{inc} relies only on $\boldsymbol{H}_{dc}$, i.e,

$$\chi_{inc}^{(\boldsymbol{H}_{dc})} = \frac{\Delta M}{\Delta H}.$$

When the exciting coil is driven by a sinusoidal voltage signal, H_{ac} can be expressed as H_{ac}=$ni\sin(2\pi ft)$ over the sample region, where n is the density of turns of the exciting coil, i is the magnitude of the current through the exciting coil, and f is the frequency of the AC current. On the basis of Faraday's law, the electromotive force of the pick-up coil can be directly calculated by

$$\begin{aligned}V_p &= -\frac{\mathrm{d}\Phi}{\mathrm{d}t} = \sum_{n'=1}^{N} -2\pi f\mu_0\left(R_{in}+n'D\right)^2 ni\cos(2\pi ft) \\ &\quad \times\left(\pi + \frac{\chi_{inc}^{(H_{dc})}v}{2(h^2+(R_{in}+n'D)^2)^{3/2}}\right).\end{aligned}$$

The sample is so far from the compensating coil that the contribution that the sample makes to the magnetic flux through the compensating coil can be ignored. Apart from the sample, the compensating coil and the pick-up coil should be located in symmetric positions with respect to the exciting coil and external electromagnet. Therefore the electromotive force of the compensating coil is

$$V_{\rm c} = \sum_{n'=1}^{N} -2\pi^2 f\mu_0 \left(R_{\rm in}+n'D\right)^2 ni\cos\left(2\pi ft\right).$$

The output of the pick-up and compensating coil, $V_{\rm p}-V_{\rm c}$, is measured by LIA, whose operating frequency is f. The magnitude of the output voltage of LIA is

$$V = \sum_{n'=1}^{N} \pi f\mu_0 \left(R_{\rm in}+n'D\right)^2 ni \frac{v\chi_{\rm inc}^{(H_{\rm dc})}}{\left(h^2+\left(R_{\rm in}+n'D\right)^2\right)^{3/2}}. \quad (1)$$

All the parameters which affect the output voltage are constants in a built ideal system except $\chi_{\rm inc}^{(H_{\rm dc})}$, which depends on$H_{\rm dc}$. Therefore, the changes of the output voltage describe proportionally the changes of $\chi_{\rm inc}^{(H_{\rm dc})}$ at different $H_{\rm dc}$($\chi_{\rm inc}^{(H_{\rm dc})} \propto V$). The $H_{\rm dc}-\chi_{\rm inc}^{(H_{\rm dc})}$ curve follows the same trend as the $H_{\rm dc}$–V curve. Because the measurement means is that $H_{\rm ac}$ is superimposed on $H_{\rm dc}$, the reversible part of the magnetization $M_{\rm rev}$ can be calculated by

$$M_{\rm rev}\left(H\right) = \int_{H_0}^{H} \chi_{\rm inc}^{(H_{\rm dc})}\,{\rm d}H + M_{\rm rev}\left(H_0\right).$$

This is an important parameter to gain the magnetization curve.

As Eq. (1) shows, the magnitude of the output voltage is affected by N, f, n, i, $R_{\rm in}$, D, v, and the distance from the sample to the pick-up coil h. The main sources of the noise are the Johnson noise of the resistors of the coils, the asymmetry between the pick-up and the compensating coil, the mismatches that happen occasionally when the resistance of exciting coil is regarded as the output impedance of the voltage source and the resistance of the pick-up and compensating coils is treated as the input impedance of the LIA. As discussed below, it is possible to increase the output signal.

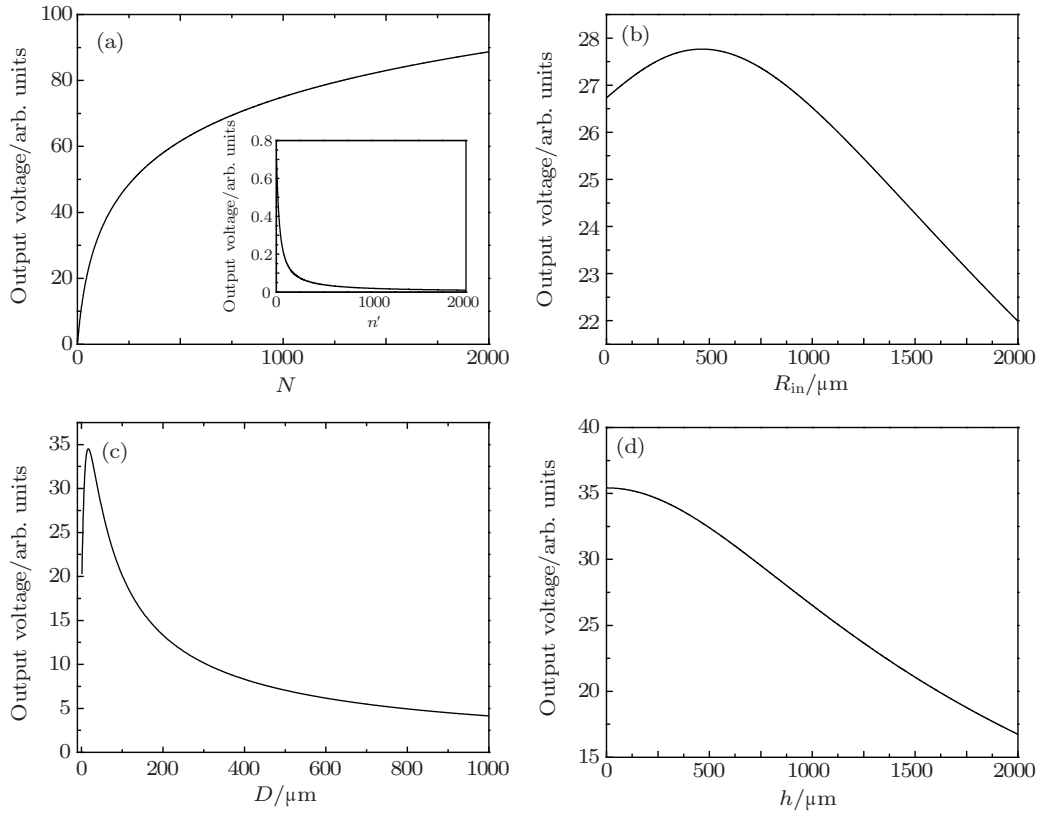


Fig. 3. Output voltage as a function of parameters of the pick-up coil: (a) the number of turns of the pick-up coil, the inset is the output voltage of n'-th turn of the pick-up coil; (b) the inner radius of the pick-up coil; (c) the diameter of the copper wire; and (d) the distance from the sample to the pick-up coil.

(i) The four parameters relative to the pick-up coil (N, $R_{\rm in}$, D, h) are independent of each other; hence, we assume the initial conditions are that $N = 100$, $R_{\rm in} = 1000$ μm, $D = 50$ μm, $h = 500$ μm, $\pi f\mu_0 niv\chi_{\rm inc}^{(H_{\rm dc})} = 1000$. Figure 3 shows the curves of the output voltage when one of the four parameters changes. When N is increased from 1 to 2000, the output volt-

age raises significantly. However, the contribution made by the increased coil to the output voltage is less when N is greater than 300. The resistance of the pick-up coil is still proportional to N, which then leads to increasing Johnson noise and the mismatch between the resistance of the pick-up coil and the input impedance of the LIA. Such a situation results in a decrease of the signal-noise ratio. Hence, it is not useful to improve the signal-noise ratio by increasing N injudiciously. Figure 3(b) shows that the output voltage curve caused by the change of the inner radius $R_{\rm in}$ is not monotone. There is the maximum output voltage at $R_{\rm in} = 464$ μm. While under the restriction of the size of the diamond, it is difficult to achieve the optimal size for $R_{\rm in}$ all the time. As is shown in Fig. 3(c), the maximum output voltage exists at $D = 17$ μm and when D is above 17 μm, the smaller the diameter D of the copper wire is, the greater the output signal becomes. However, a small diameter of the copper wire also could cause an increase of the resistance of the pick-up coil. The output voltage decreases significantly, as the distance from the sample to the pick-up coil increases (Fig. 3(d)) Therefore decreasing h is an effective method to improve the output voltage, but it is impractical to reduce h unboundedly due to the limitation of the diamond. The analysis of the four parameters that affect the output voltage is only in theory, yet the reality is quite complex. Generally the initial conditions are adopted according to practical constraints, and then the parameters are adjusted by Eq. (1) as a reference.

(ii) In fact, the compensating coil may not offset the background signal fully, so the output signal may also include some residual background noise. The output voltage rises with the increase of the density of turns of the exciting coil n. Reducing the diameter of the copper wire of the exciting coil is the only method to increase n; however at the same time the resistance of the exciting coil increases quadratically. This results in the Johnson noise of the exciting coil also increasing quadratically. When increasing the frequency of exciting current f and the magnitude of the exciting current i, the background noise also increases. Figure 4 shows the sample signal experimental data and the sample-to-background signal ratio (STBR) curve under different exciting frequencies and currents. To obtain an obvious signal, a relatively big sample is selected. The output voltage of the sample increases linearly with the increase of f and i. However the STBR increases disproportionately.

(iii) Increasing the volume of the sample is the most effective means to improve the output voltage. However, the size of the sample chamber of the DAC is too small to allow a sample that is as big as we would prefer.

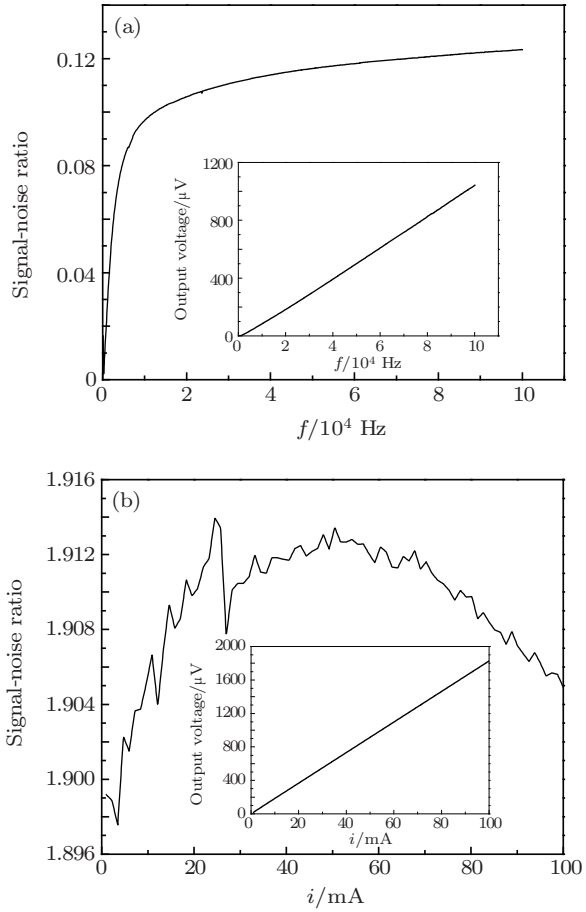


Fig. 4. The STBR as a function of exciting frequency and current: (a) the STBR under different exciting frequencies (sample signal shown in the inset); (b) the STBR under different exciting currents (sample signal shown in the inset).

3. Experimental results

The measurement system is based on a titanium alloy DAC that can impose pressure less than 25 GPa. The number of the turns of the pick-up and compensating coils, made with 40 μm pure copper wire, is 250. The inner diameter and the thickness of them are 1.5 mm and 0.5 mm. The 300-turn exciting coil is made of constant enameled wires with a diameter of 80 μm, wound around the pick-up and compensating coils. The inner diameter and the thickness of exciting coil are 10 mm and 1 mm. When a sinusoidal voltage of 5 V peak and 4.7 kHz frequency is applied to the exciting coil, it produces a peak ac magnetic field of 1 Oe over the sample region. An external magnetic field varying from −0.9 T to 0.9 T is produced by an electromagnetic. The iron sample is located in the sample chamber whose size is about 140 μm wide and 70 μm deep, cut in a tungsten gasket. The output voltage is measured by a SIGNAL RECOVERY Model 7265 lock-in amplifier. The output voltage of the iron sample is about 5 μV while the noise of LIA is about 0.01 μV. The minimum size of the sample that the measurement system can distinguish is about $25 \times 25 \times 70$ μm^3 and the output voltage of the minimum sample is 0.17 μV with 0.01 μV noise. Pressure is determined by

the shift in the ruby R_1 peak.[28] When pressure on the sample increases, the sample cycles through external magnetic field H_{dc} of ± 0.9 T to obtain χ_{inc} (P, H_{dc}) and the H_{dc}–χ_{inc} (P, H_{dc}) curve L_1 (Fig. 5(a)). To avoid the interference of background noise, the H_{dc}–χ_{inc} curve L_2 (Fig. 5(a)) of the empty gasket under the same condition is measured. Then curve L_2 is subtracted from curve L_1 to obtain the curve L_3 (Fig. 5(a)), which characterizes the trend of χ_{inc} as a function of H_{dc}. The integral of curve L_3 is the magnetization curve of iron sample (Fig. 5(b)). The same steps are applied to the H_{dc}–χ_{inc} curve under different pressures. Figure 6 shows the P–H_{dc}–χ_{inc} 3D image and figure 7 shows the magnetization curves. The other two samples of different sizes are measured, and the results are almost the same as that shown in Fig. 6, except the magnitudes of χ_{inc}.

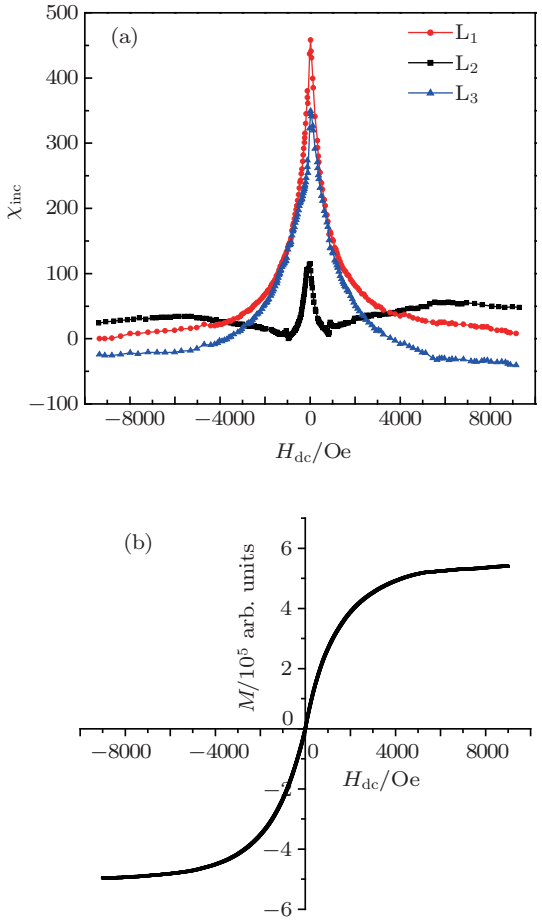


Fig. 5. (color online) (a) The χ_{inc} curve under different H_{dc} of sample + gasket (L_1), gasket (L_2) and sample (L_3); (b) the integral of L_3.

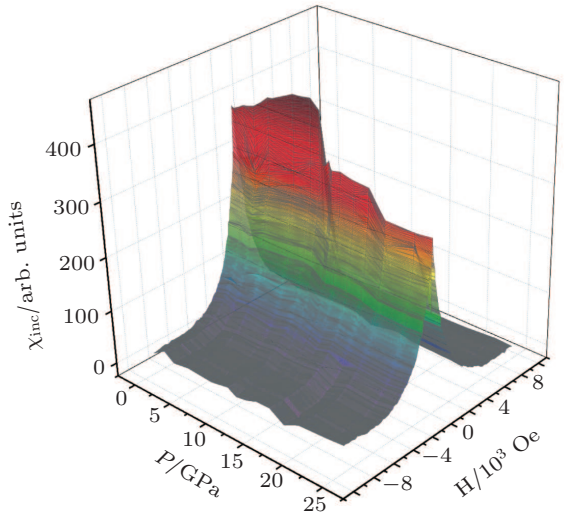


Fig. 6. (color online) P–H_{dc}–χ_{inc} 3D image.

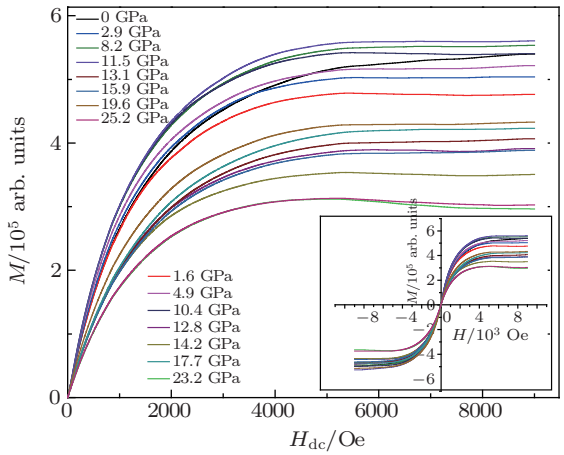


Fig. 7. (color online) Magnetization curves under different pressures from 0 to 0.9 T Inset shows the magnetization curves under different pressures from -0.9 T to 0.9 T.

4. Discussion and conclusions

The saturation magnetizations under different pressures are shown in Fig. 8. When pressures are below 11.5 GPa, the shapes of the magnetization curves are almost the same, with high Ms. From 11.5 GPa to 12.8 GPa, Ms decreases 30% and χ_{inc} at 12.8 GPa are less than that at 11.5 GPa, as Fig. 6 shows. This implies that the sample undergoes a magnetic transition. During the transition the bcc and hcp coexist.[26] Compared to Ms at atmospheric pressure, Ms is reduced by 45% at 19.6 GPa and it tends to reach a constant value above 19.6 GPa. This signifies that the magnetic transition ends at 17.7–19.6 GPa, and this transition occurs during an increment of 5–8 GPa. The trend of Ms is consistent with the abundance of

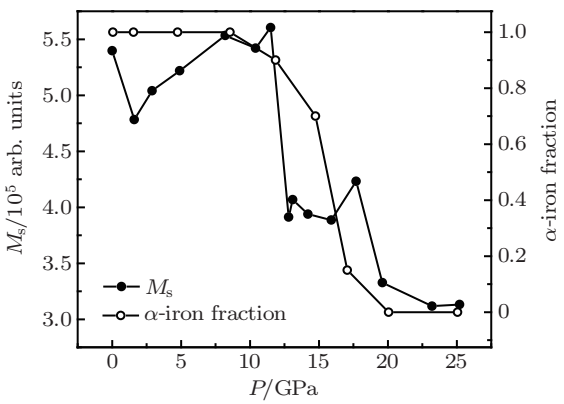


Fig. 8. The saturation magnetization and the abundance of α-iron fraction under different pressures. Open circle: M_s; filled circle: the abundance of α-iron from Taylor *et al.*[21]

α-iron as a function of pressure, determined from Mössbauer spectroscopy by Taylor *et al.*[21] The iron exists in hcp state above 16 GPa.[22,24,26] The data show that above 19.6 GPa the sample also displays hysteresis, but the magnetic susceptibility is about 45% less than the initial status at atmospheric pressure. This suggests that hcp iron is either initially ferromagnetic or paramagnetic.

Acknowledgment

We thank Huang Feng-Xian, Huang Xiao-Li, Liu Ran, and Wu Gang for facilitating the high pressure experiment.

References

[1] Struzhkin V V, Hemley R J, Mao H K, Timofeev Y A and Eremets M I 2000 *Hyperfine Interactions* **128** 323
[2] Meng X X, Fan J, Bao K, Li F F, Huang X L, Li Y, Tian F B, Duan D F, Jin X L, Zhu P W, He Z, Zhou Q, Gao C X, Liu B B and Cui T 2014 *Chin. Phys. B* **23** 16102
[3] Jing Q M, Wu Q, Liu L, Bi Y, Zhang Y, Liu S G and Xu J A 2012 *Chin Phys. B* **21** 106201
[4] Jayaraman A 1983 *Rev Mod Phys* **55** 65
[5] Timofeev Y A, Struzhkin V V, Hemley R J, Mao H K and Gregoryanz E A 2002 *Rev Sci Instrum* **73** 371
[6] Kim C C, Reeves M E, Osofsky M S, Skelton E F and Liebenberg D H 1994 *Rev Sci Instrum* **65** 992
[7] Timofeev Y A, Mao H K, Struzhkin V V and Hemley R J 1999 *Rev Sci Instrum* **70** 4059
[8] Alireza P L and Julian S R 2003 *Rev Sci Instrum* **74** 4728
[9] Jackson D D, Aracne R C, Malba V, Weir S T, Catledge S A and Vohra Y K 2003 *Rev Sci Instrum* **74** 2467
[10] Yu Y, Zhai G J and Jin C Q 2009 *Chin Phys Lett.* **26** 026201
[11] Hu T L, Wang X, Han B, Li Y, Huang F X, Zhou Q and Zhang T 2013 *Chin. Phys. B* **22** 120701
[12] Ma Y Z, Somayazulu M, Shen G Y, Mao H K, Shu J F and Hemley R J 2004 *Phys. Earth Planet. Inter.* **143** 455
[13] Ekman M, Sadigh B, Einarsdotter K and Blaha P 1998 *Phys. Rev. B* **58** 5296
[14] Friák M and Šob M 2008 *Phys Rev B* **77** 174117
[15] Johnson D F and Carter E A 2008 *J Chem Phys* **128** 104704
[16] Lizárraga R, Nordström L, Eriksson O and Wills J 2008 *Phys Rev B* **78** 064410
[17] Liu J B and Johnson D D 2009 *Phys Rev B* **79** 134113
[18] Yang S, Bao H X, Zhou C, Wang Y, Ren X B, Song X P, Yoshitaka M, Yoshio K, Masahiko T and Keisuke K 2013 *Chin Phys B* **22** 046101
[19] Pipkorn D N, Edge C K, Debrunner P, De Pasquali G, Drickamer H G and Frauenfelder H 1964 *Phys Rev* **135** A1604
[20] Saburo N, Tetsuya S, Takateru K, Toshio T and Shoichi E 2002 *J Phys: Condens. Mat* **14** 11167
[21] Taylor R D, Pasternak M P and Jeanloz R 1991 *J Appl Phys.* **69** 6126
[22] Baudelet F, Pascarelli S, Mathon O, Itie J P, Polian A, d'Astuto M and Chervin J C 2005 *J Phys.: Condens Mat* **17** S957
[23] Rueff J P, Krisch M, Cai Y Q, Kaprolat A, Hanfland M, Lorenzen M, Masciovecchio C, Verbeni R and Sette F 1999 *Phys Rev B* **60** 14510
[24] Wang F M and Ingalls R 1998 *Phys Rev B* **57** 5647
[25] Monza A, Meffre A, Baudelet F, Rueff J P, d'Astuto M, Munsch P, Huotari S, Lachaize S, Chaudret B and Shukla A 2011 *Phys Rev Lett* **106** 247201
[26] Mathon O, Baudelet F, Itie J P, Polian A, d'Astuto M, Chervin J C and Pascarelli S 2004 *Phys. Rev. Lett.* **93** 255503
[27] Gilder S and Glen J 1998 *Science* **279** 72
[28] Adams D M, Appleby R and Sharma S K 1976 *J Phys E: Sci Instrum.* **9** 1140